Analysis of Temporal Polarization Phase Difference for Major Crops in India

Dipanwita Haldar[1, *], Anup Das[1], Manoj Yadav[2], Ramesh S. Hooda[2], Shiv Mohan[3], and Manab Chakraborty[1]

Abstract—A polarimetric radar system measures the complete scattering matrix of a target in the backscattered field that includes magnitudes of linearly polarized scattering amplitudes and the co-polarised and cross-polarised phase angles. Apart from backscattering intensity, the co-polarization phase difference (CPD) calculated from polarimetric synthetic aperture radar (SAR) data produces important information about target physical, geometrical and dielectric properties. In the present work, the distribution of CPD in C-band polarimetric SAR data corresponding to major *kharif* and *rabi* crops (denoting the monsoon and the winter season) and other land cover features have been studied over Central State Farm, Hisar, Haryana. The probability density functions (PDF) of CPD have been compared with dominant scattering contributions from these targets as obtained from polarimetric target decompositions. The results show that crops and other land cover features show characteristic CPD distributions, which relates well with crop physical and geometrical properties. An intuition of the rate of growth and plant vigour is indicative from the temporal PDF pattern.

1. INTRODUCTION

Discrimination of crops from other land cover classes and crop classifications are very important activities in India for agricultural monitoring and timely forecasting of crop production. In this regard, airborne as well as space-borne remote sensing data particularly Synthetic Aperture Radar (SAR) data has shown promising results in crop monitoring and classification with reasonably high accuracy. While several authors have reported the use of SAR backscatter coefficient in different polarizations and frequencies for crop identification and monitoring [10–14], several others have reported using polarimetric scattering matrix that contains information about polarization amplitude as well as phase for crop characterization and classification [6, 15–19]. Some authors have attempted to establish relationships between polarization phase differences of SAR signals to target properties [1–3]. These studies show that the relative phase angles of polarized SAR signals are dependent on the physical, dielectric and geometrical properties of targets and distribution of polarization phase angles over natural distributed targets provide useful information about target properties.

1.1. Polarization Phase Difference (PPD)

A coherent polarimetric SAR system measures the complete scattering matrix of a pixel in the backscattered field. For a linear polarization mono-static SAR that coherently transmits and receives in both horizontal (h) and vertical (v) polarizations, when scattering reciprocity is assumed (i.e., $S_{hv} = S_{vh}$), the scattering matrix S can be written in the form [4, 5, 7]

$$S = e^{i\phi_{vv}} \begin{bmatrix} |S_{vv}| & |S_{vh}| e^{i\phi_X} \\ |S_{vh}| e^{i\phi_X} & |S_{hh}| e^{i\phi_C} \end{bmatrix} \tag{1}$$

where $|S_{pq}|$ is the magnitude of the complex scattering amplitude S_{pq} (for p, $q = v$ or h), and ϕ_{pq} is the phase angle. $\phi_X = \phi_{hv} - \phi_{vv} = \phi_{vh} - \phi_{vv}$ and $\phi_C = \phi_{hh} - \phi_{vv}$ are the phase angles relative to ϕ_X, and ϕ_C are called cross and co-polarization phase angles (or differences), respectively.

For most natural targets, the cross-polarization phase difference ϕ_X is uniformly distributed over $[-180°, +180°]$, and therefore contains no target specific information. On the other hand, the co-polarization phase difference (CPD) ϕ_C has a Gaussian probability density function (PDF), which is strongly dependent on both the target parameters (roughness, dielectric constant, geometry etc.) and the radar parameters (incident angle and frequency) [2]. For mono-static SAR system and in backscattering alignment (BSA) convention, an ideal odd-bounce (smooth dielectric surface) scatterer will have a CPD of 0°, while an ideal even-bounce (dihedral) scatterer will have a CPD of ±180°. For diffuse type of scattering, the CPD values are variable.

Figure 1 shows the expected PDF of the co-polarized phase difference for some natural targets; (a) smooth surface, (b) rough surface, (c) dense vegetation and (d) buildings. The PDF of ϕ_C can be characterized by the mean CPD and standard deviation of CPD, which is a measure of the correlation between the two co-polarized scattering amplitudes and is represented by the width of the PDF [7, 20]. For most of the pure targets the mean CPD value is close to 0°. For a very smooth surface, the width of the PDF is expected to be very low as there is high correlation between the HH and VV amplitudes (Fig. 1(a)). As the roughness increases, assuming identical soil moisture condition, the width of the PDF is expected to increase (Fig. 1(b)) as more number of facets and scatterers will contribute to the CPD. Similarly, for randomly oriented dipoles or diffused scatterers such as dense vegetation, the PDF of CPD is expected to be uniformly distributed over the range $[-180°, 180°]$ due to total un-correlation between HH and VV amplitudes (Fig. 1(c)). This is because, when the multiple reflections from randomly oriented dipoles are added, it is equally probable that they may add in phase or out of phase. For dihedral (or even bounce) type scatterers such as floor-wall planes of buildings the CPD values will be close to ±180° and the expected PDF is as shown in Fig. 1(d). The following figure is drawn based on the inferences of the standard scattering mechanisms.
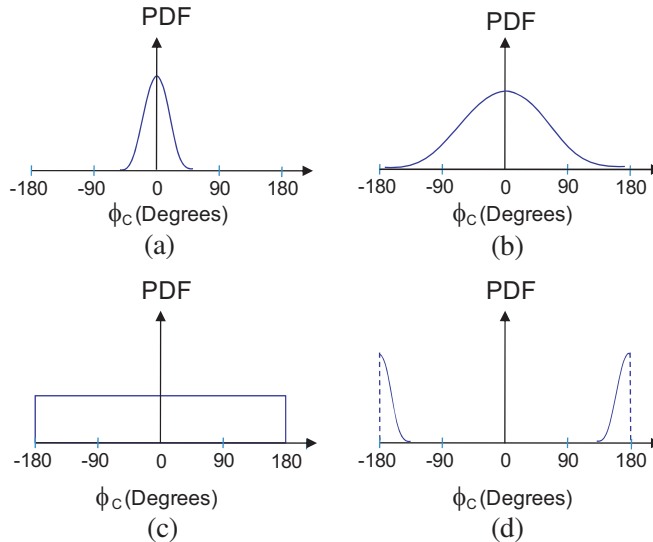
Figure 1. Expected probability density function (PDF) of the co-polarized phase difference for (a) smooth surface (odd bounce scattering), (b) rough surface (Bragg scattering), (c) dense vegetation (volume or diffused scattering) and (d) buildings (even-bounce scattering).

For all natural targets spreading across several pixels in a SAR image, the PDF of CPD is expected to be a combination of these PDFs. In the present study, the temporal CPD distributions of major *kharif* and *rabi* crops and other associated land cover features over Central State Farm, Hisar, Haryana have been analyzed and the characteristics of CPD distributions have been related with the crop biophysical

and geometrical parameters. The implications to crop phenology are also related to the progress of PPD. The results have also been compared with dominant scattering mechanisms associated with the features as obtained from modified Freeman-Durden decomposition [9] modified from [8].

2. STUDY AREA AND DATASETS

Central State Farm located in Hisar district of Haryana (India) has been selected for the present study. The area lies between the coordinates 29°11′-29°20′N latitudes and 75°36′-75°45′E longitudes. This is a farmland of considerable size where large experimental crop fields (more than 5 hectares) are maintained for seed generation and distribution to the state farmers. The major agricultural crops grown in this area include paddy, cotton and pulses during Indian *kharif* (summer/monsoon) season and wheat, mustard, gram, peas during Indian *rabi* (winter) season. This site was selected for developing methodology for crop discrimination and classification using polarimetric SAR data from Radarsat-2. Some of the cluster villages are surrounded by water bodies (ponds).

Multi-date, C-band single-look complex (SLC) data have been used for this study. In SLC data, each resolution cell of the image, called pixel is characterized by amplitude value (represents the strength of the returned signal) and an absolute phase value (represents the time delay of the received signal in a coherent system), both are jointly represented as a 'complex number'. Polarimetric SAR data were acquired on different dates over crop calendars. Details of SAR data are given in Table 1 below. All the seven scenes were acquired between July 2010 and March 2011 coinciding *kharif* and *rabi* cropping seasons with wheat, mustard, gram as predominant *rabi* crops and paddy, cotton, guar as predominant *kharif* crops.

Table 1. Details of Radarsat-2 data used in this study.

Sl. No.	Polarization	Central Inc. Angle	Acquisition Mode and beam	Ground Range Pixel spacing	Date of Acquisition: dd/mm/yyyy
1	Full: HH, HV, VH, VV	40°	Descending, right looking FQ21	6 m	04/07/2010
2	-do-	-do-	-do-	-do-	21/08/2010
3	-do-	-do-	-do-	-do-	08/10/2010
4	-do-	-do-	-do-	-do-	24/12/2010
5	-do-	-do-	-do-	-do-	17/01/2011
6	-do-	-do-	-do-	-do-	06/03/2011
7	-do-	-do-	-do-	-do-	31/03/2011
-do-	Indicates same specifications as above				

Apart from the crops, two other landuse classes *viz.* bare soil and built-up area (or human settlements) those were present in the study area were also included for present study. Synchronous ground truth information including vegetation and soil parameters viz. sowing date, crop stage, method of sowing, row-spacing for row crops, plant density, plant height, leaf area, crop vigour, expected date of harvest, background soil, soil type, soil moisture, field size etc. corresponding to the date of acquisitions of all the SAR data were collected for subsequent analysis.

3. METHODOLOGY

Radarsat-2 polarimetric SAR data as level-1 SLC product were imported in PCI-Geomatica® image processing software. The Radar Analysis Tool (RAT) has also been used for data analysis purpose [21].

The co-polarization phase difference was calculated from the complex numbers depicting the co-polarized scattered signals (S_{hh} and S_{vv}) as follows [1, 2]:

$$\phi_C = \varphi_{hh} - \varphi_{vv} = \left\langle \tan^{-1}\left(\frac{\Im(S_{hh})}{\Re(S_{hh})}\right) - \tan^{-1}\left(\frac{\Im(S_{vv})}{\Re(S_{vv})}\right) \right\rangle \tag{2}$$

where, '$\Im$' denotes the imaginary part; '$\Re$' denotes the real part and $\langle\cdot\rangle$ denotes the spatial averaging over a group of neighboring pixels. φ_{hh} and φ_{vv} are physically equivalent to absolute phases. The SPAN image has been generated in PolSARPro [22]. The modified Freeman-Durden decomposition (2007) [9] a modified version of the first theory [8] has been applied to partition the area to dominant scattering mechanisms.

4. RESULTS AND DISCUSSIONS

The CPD of various *kharif* and *rabi* landcovers were plotted, analysed and interpreted with respect to surroundings. The phenology of crop growth progress is interpreted through these PPDs. The various dominant scattering mechanisms, i.e., double bounce (D-b), volume (Vol) and surface (Sur) in percentage have been quantified from the modified Freeman-Durden decomposition.

4.1. Discussion on *Kharif* (Rainy Season) Crops and Other Landcovers

The **urban** structure due to dominance of double bounce scattering has a frequency distribution almost uniformly randomized across the ends, i.e., −180 to +180 degrees. In early July data due to lesser developed background, i.e., the surrounding *kharif* crop, there is random equi-distribution kind of pattern for the urban features (Fig. 2). As the surrounding crop growth progress the frequency distribution takes a near U-shaped entity with minimum frequency distribution near zero. Increasing both ways from zero value, the maximum frequency distribution corresponds with the −180 and +180 (Fig. 2).

Table 2 shows the number of samples and mean CPD of the crops in kharif with time series analysis. The mean PPD is having highest range in paddy; around 12 in July to 7 in August and −3 in October it is an indicative of the dynamic temporal profile. Cotton shows change in sign from July to August due to uneven surface to volume scattering.

Table 2. Distribution of sample size, mean, median and standard deviation of co-polarized phase difference (CPD) across various land cover classes during *kharif* season.

Date of SAR observation	Land cover	No of samples (N)	Mean CPD (degree)	Median (degrees)	Standard deviation
04 July, 2010	Cotton	398	1.7	3.5	56.6
	Paddy	341	12.4	4.4	48.7
	Guar	477	3.0	1.4	50.3
	Fallow	223	−2.1	−8.0	38.6
	Urban	830	−7.5	−0.3	107.8
21 August, 2010	Cotton	417	−2.9	0.5	81.6
	Paddy	339	7.2	−2.2	71.7
	Guar	551	−1.3	0.5	77.8
	Fallow	259	3.4	−0.8	74.4
	Urban	645	−0.02	−0.1	122.9
08 October, 2010	Cotton	256	−4.2	1.3	74.3
	Paddy	567	−3.0	0.6	65.7
	Guar	698	−1.4	−1.4	64.2
	Fallow	443	−1.7	2.2	52.3
	Urban	527	−12.0	−1.3	120.3
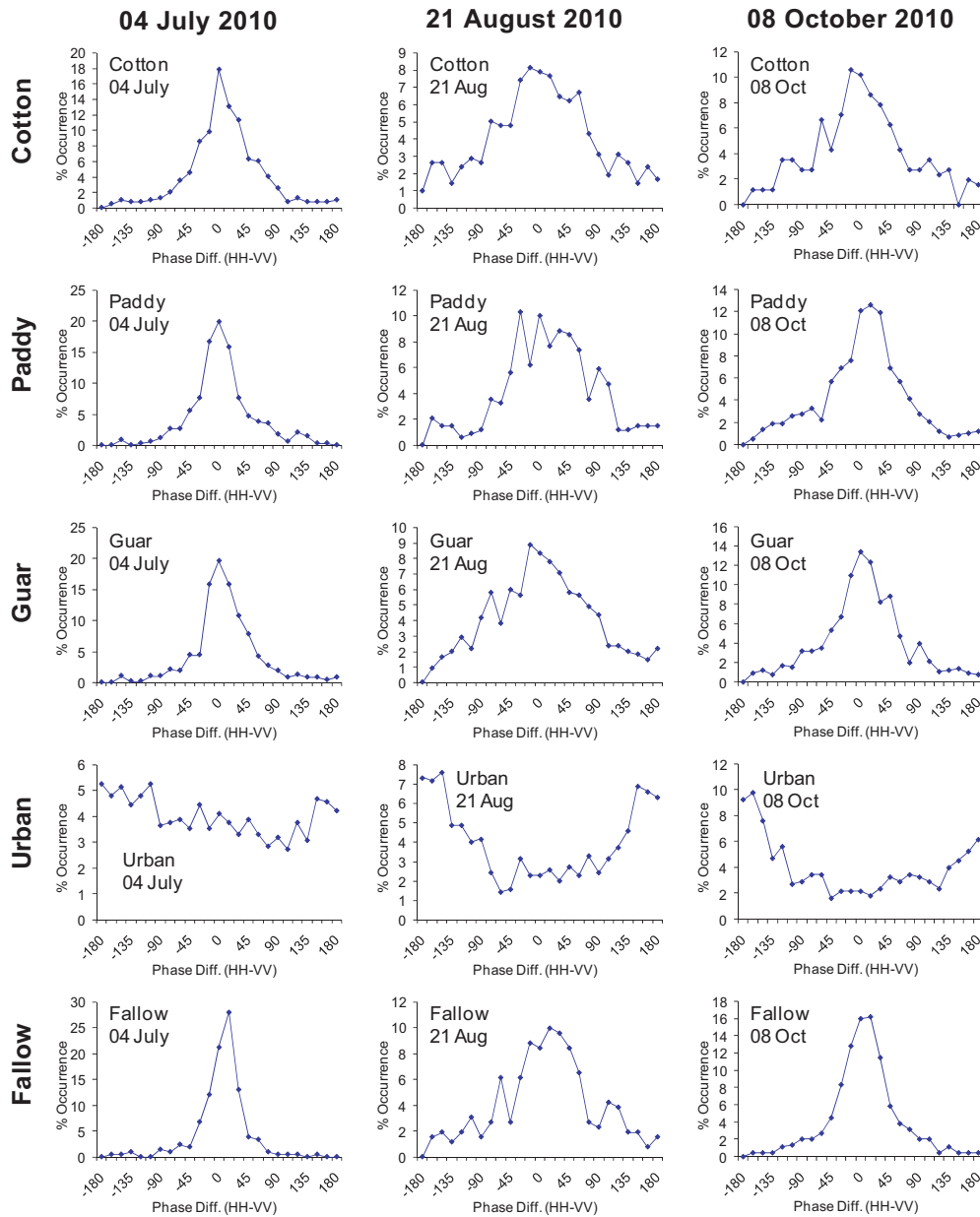
Figure 2. CPD distribution (in degrees) for major *Kharif* crops and land cover features in the central state farm region during July, August and October, 2010.

The fallow plots frequency distribution in early July shows a signature close to bare soil. This resemblance is due to the bare nature of the fallow due to absence of vegetation at the onset of monsoon. Fallow at end of the *kharif* season consists of bare soil plus some fields with natural vegetation. This growth of vegetation will increase the frequency distribution away from zero indicating presence of current fallow in *rabi* getting natural vegetation cover in *kharif*. As can be seen from the analysis of Freeman-Durden Decomposition, the current fallow has the highest surface scattering at the beginning of the season (Fig. 2 and Fig. 5). With onset of monsoon the natural vegetation grows up by August–September and the percent contribution by volume scattering increases subsequently.

The major crops in *kharif* season are paddy, cotton and guar. Paddy is transplanted mostly in end June to first week of July in this area. Only at few places, the transplantation is delayed to 2nd–3rd week of July.
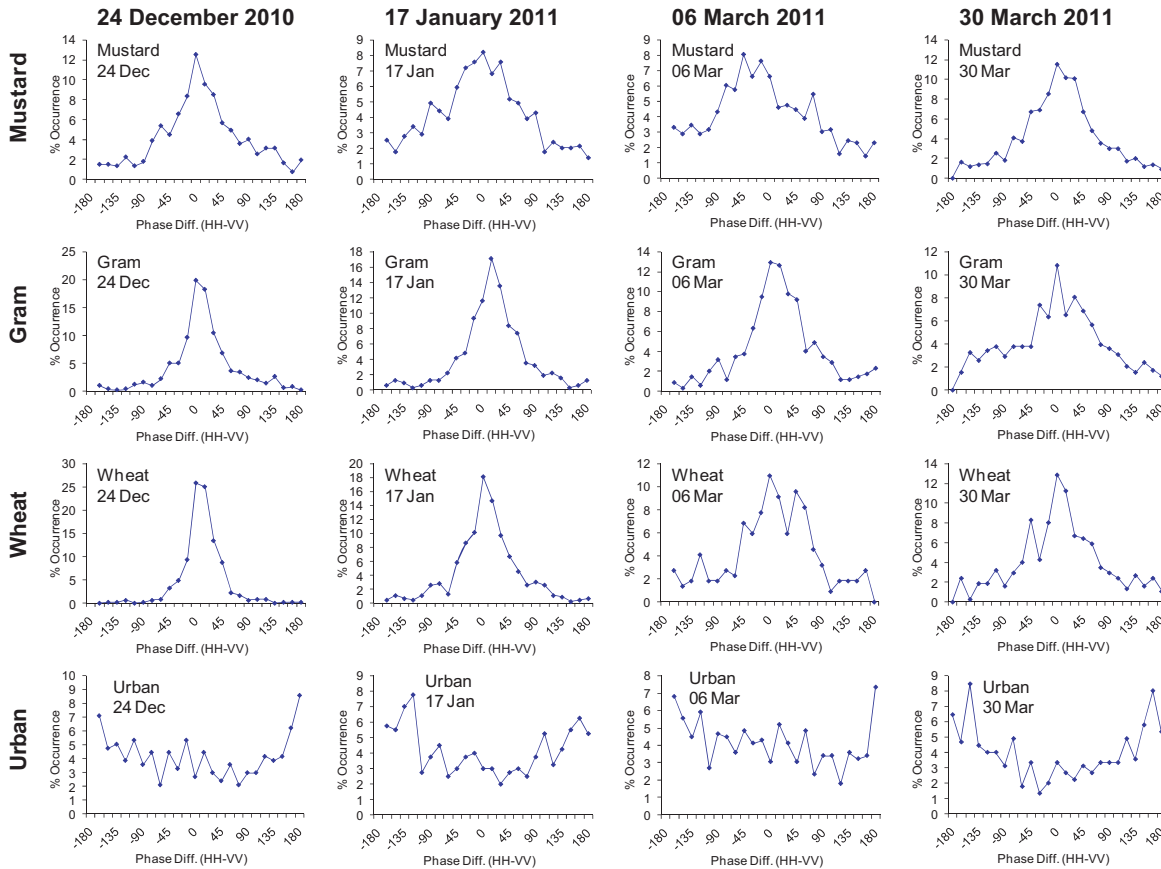
Figure 3. CPD distribution (in degrees) for major *Rabi* crops and land cover features in the central State farm region during December 24, January 17, March 06 and March 30.

Thus surface scattering dominates in the first week of July due to standing water with just transplanted seedlings or ongoing transplantation process. By end August-early September the crop reaches the peak vegetative stage which gets reflected as dominance of volume scattering with suppressed surface scattering and negligible double bounce scattering. Some amount of double bounce scattering is observed in the intermediate stage when the crop stands erect over the water surface with vertical plant component dominating the scattering process. During October harvest starts, bringing back the CPD distribution narrow with zero (0) centric (Fig. 2)

Cotton is a long duration *kharif* crop sown in north India prior to the onset of monsoon in end April to early May with one pre-sowing irrigation. In few places where irrigation is a constraint, the sowing may be delayed till end of May. Cotton is a very slow growing crop particularly in the beginning of the season. As seen from the following table of Freeman-Durden decomposition, during early July, surface scattering dominates but some (20%) volume scattering component is present which is higher than paddy which is just transplanted (Table 3). During end August to early September, cotton is in peak vegetative stage with ball formation initiated. Paddy is also in peak vegetative stage during end August to early September with dominance of volume scattering. By 2nd week of October paddy is in maturity stage with onset of harvest in majority of the parts. Thus 8th October data shows decrease in volume scattering and increase in surface scattering component predominantly for paddy and also to some extent in cotton (Table 3). In case of cotton the volume scattering component reduces by 2nd week of October due to completion of two picking and also yellowing, drying and fall of lower leaves (Fig. 2)

Guar is an important fodder and gum source crop grown over an appreciable area in the north-western region particularly Haryana and Rajasthan. It is late sown as compared to cotton or paddy, normally sown during mid July. It is fast growing crop as compared to cotton. By end August volume

scattering component dominates. By end September-early October some of the full grown guar crop is harvested for fodder use thus reducing the volume scattering component only slightly in October, as all fields are not harvested together, harvest continues in phases as per the requirement (Fig. 2, Table 3). In October some of the fields are harvested. Thus the October data shows decreased volume scattering and some translation to surface scattering. Thus the signature is nearly similar though not exactly thus shows predominance of surface scattering in July but equal proportion of both in October.

Table 3. Percentage contribution of various scattering mechanism based on modified Freeman-Durden decomposition from different targets during *kharif* (monsoon) season.

Date of pass	04 July, 2010			21 August, 2010			08 October, 2010		
Scattering mechanism	D-b	Vol.	Sur.	D-b	Vol.	Sur.	D-b	Vol.	Sur.
Cotton	5.49	20.79	73.71	6.32	58.36	36.25	9.85	46.85	43.30
Paddy	4.09	13.66	82.25	4.99	63.66	32.20	11.64	30.10	58.26
Guar	4.93	11.17	83.90	8.90	46.17	42.90	11.11	40.12	48.77
Fallow	2.20	7.30	90.50	4.20	19.30	73.50	5.82	17.42	76.76
Urban	63.34	12.55	24.11	83.33	2.55	14.11	90.10	1.99	7.91

∗D-b: Double bounce; Vol.: volume; Sur: Surface

4.2. Discussion on *Rabi* (Winter) Crops

The winter crops sown in this region are mustard, wheat and gram mostly with some pockets of pea, *rabi* jowar, etc. Mustard is the earliest to be sown mostly form the end of September to mid October. It has appreciable growth by mid December with significant amount of volume scattering though surface scattering still has around 50% of contribution to the total scattering. By mid January, volume scattering component dominates during the peak vegetative stage. Further the volume scattering component increases and continues till first week of March, thereafter decreases with leaf shedding, pod maturity

Table 4. Distribution of sample size, mean, median and standard deviation of co-polarized phase difference (CPD) across various land cover classes during *rabi* season.

Date of SAR observation	Land cover	No of samples (N)	Mean CPD (degree)	Median (degrees)	Standard deviation
24 December, 2010	Mustard	672	3.4	−0.8	74.2
	Gram	499	6.04	−5.3	54.6
	Wheat	491	4.6	8.6	34.3
	Urban	338	−0.5	0.3	115.6
17 January, 2011	Mustard	792	−8.5	0.3	82.1
	Gram	310	10.7	−1.8	58.1
	Wheat	464	−0.8	−0.2	55.1
	Urban	400	−4.8	−0.2	115.4
06 March, 2011	Mustard	696	−14.8	0.3	86.9
	Gram	348	9.4	−0.9	66.0
	Wheat	219	−2.1	−6.0	75.5
	Urban	559	−10.2	0.1	109.5
30 March, 2011	Mustard	1100	−0.7	0.1	70.2
	Gram	580	−5.3	1.5	81.4
	Wheat	367	2.7	4.5	71.7
	Urban	421	4.0	0.04	119.1

and start of harvest. Gram is sown mostly during 2nd week of November; it is sown mostly in ridges. Most of its growing phase witnesses a wide extent of field exposure. From December to end March data show dominance of surface scattering with rise in volume scattering only in early March. The scattering signature thus supports the slow growth habit of gram contrary to mustard (Fig. 3, Table 5).

Wheat is the latest crop to be sown mostly in end November to early December generally after the harvest of cotton. Surface scattering dominates in December–January data. From end February onwards, the volume scattering component increases due to rapid vegetative growth. 6th March data shows dominance of volume scattering in wheat which reduces by end March onwards due to maturity and harvest in end April (Fig. 3, Table 5). Table 4 shows the number of samples and mean CPD of the crops in rabi with time series analysis.

The nearby water bodies show dominance of surface scattering in all the dates in both *kharif* and
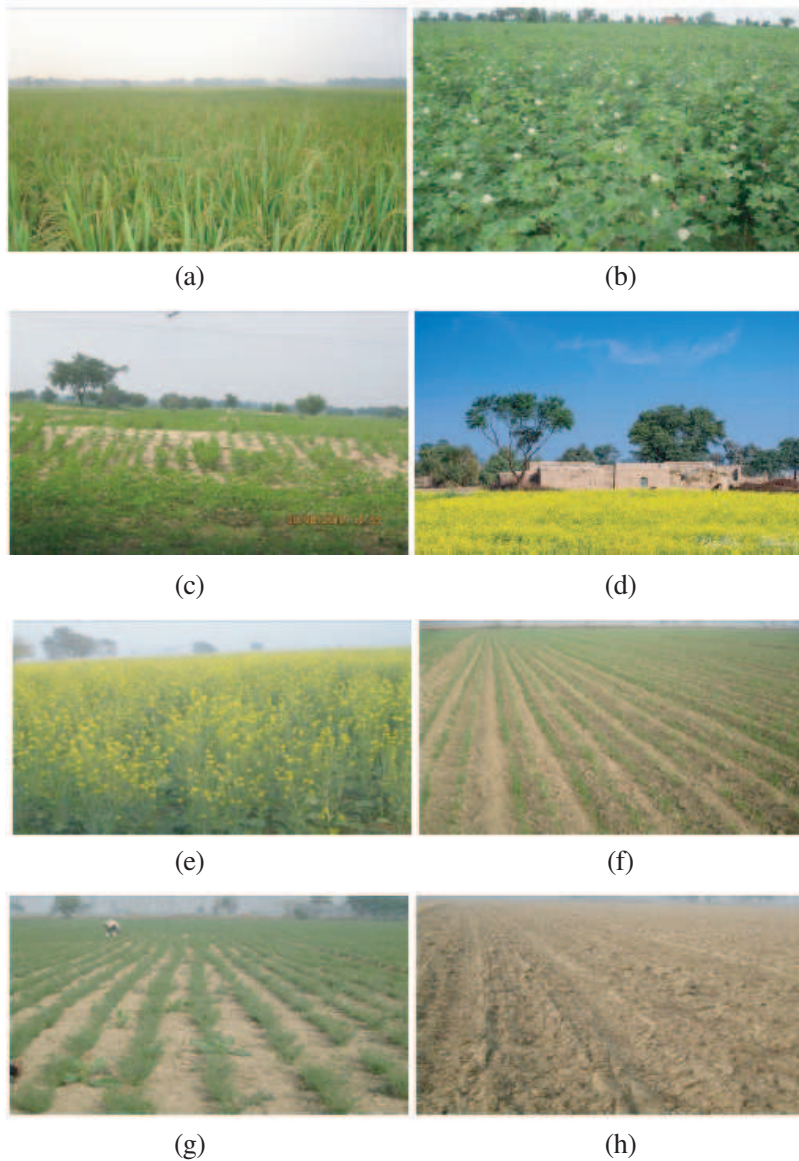
Figure 4. (a)–(h) Field photographs of various crops of *Kharif* and *Rabi* season: (a) paddy crop with panicles, (b) cotton crop in peak flowering stage, (c) Guar in early vegetative stage, (d) rural settlement adjoining the mustard fields, (e) mustard in peak flowering stage, (f) wheat in early tillering stage, (g) gram in vegetative stage, (h) recent ploughed fallow land prepared for next crop.

Table 5. Percentage Contribution of various scattering mechanism based on modified Freeman-Durden decomposition from different targets during *rabi* (winter) season.

Date of pass	**24 December, 2010**			**17 January, 2011**			**06 March, 2011**			**31 March, 2011**		
Scattering mechanism (in percent)	D-b	Vol.	Sur.	D-b	Vol.	Sur.	D-b	Vol.	Sur.	D-b	Vol.	Sur.
Mustard	10.32 2	36.31	53.36	13.13	46.72	40.15	13.56	55.45	30.99	10.17	33.42	56.41
Gram	6.80	21.00	72.20	6.59	23.11	70.30	7.08	37.40	55.52	16.17	37.78	46.05
Wheat	2.20	5.86	91.94	6.88	11.79	81.33	10.87	40.80	48.33	9.92	30.23	59.85
Urban	69.85 5	5.27	24.88	83.19	6.04	10.77	54.66	14.74	30.60	84.71	3.25	12.04

*D-b: Double bounce; Vol.: volume; Sur: Surface
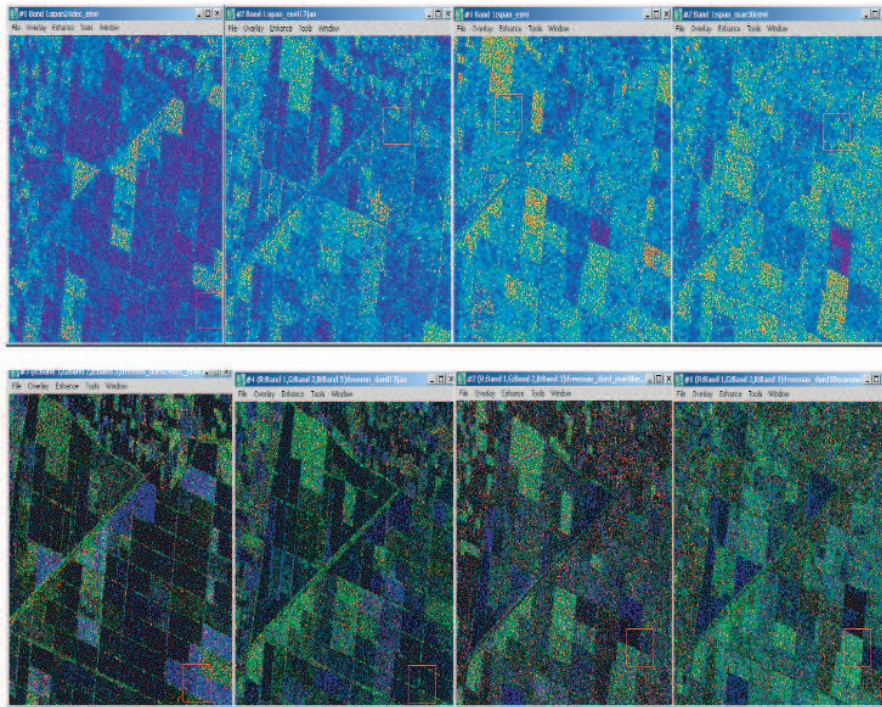
Figure 5. The SPAN image of December 24, January 17, March 06 and March 30 in sequence; corresponding modified Freeman-Durden decomposition result demonstrating increased volume and double bounce scattering during December 24, 2010–March 30, 2011.

rabi season. The modified Freeman-Durden decomposed image used in the study is shown in Fig. 5 the slow transformation of the surface scattering to volume scattering showing the progress of crop growth is seen in the figure.

In the rabi season due to assured irrigation in this area no dominant fallow fields were observed.

Field photographs of the important landcover types of study area are shown in Fig. 4.

The SPAN and Freeman images in the Fig. 5 show increase in total power in March from December onwards. Green areas shows the SAR detected spread of mustard crop in January image. Moist-zones

where wheat crop has been sown appear red in December image. The green patch in March 30 which is absent in January image shows the progress of wheat growth which is late by around 2 months after mustard.

5. CONCLUSIONS

The distribution of CPD in C-band polarimetric SAR data corresponding to major *kharif* and *rabi* crops and other land cover features have been studied over Central State Farm, Hisar, Haryana. The probability density functions (PDF) of CPD have been compared with dominant scattering contributions from these targets. The results show that crops and other land cover features show characteristic CPD distributions, which relates well with crop physical and geometrical properties. An apprehension of the rate of growth and plant phenology is indicative from the temporal PDF pattern. The biomass variation in the same crop type as well as the crop calendar can be inferred and related to the PPD distribution pattern as well as the decomposition techniques. The conjunctive use of these two techniques can help us in zonating the crop strata based on their phenology, structure and vigour.

ACKNOWLEDGMENT

REFERENCES

1. Ulaby, F. T., D. Held, M. C. Dobson, K. C. McDonald, and B. A. Thomas, "Relating polarization phase difference (PPD) of SAR signals to scene properties," *IEEE Transactions on Geosci. and Remote Sensing*, Vol. 25, No. 1, 83–91, 1987.

2. Boerner, W. M., B. Y. Foo, and H. J. Eom, "Interpretation of the polarimetric co-polarization phase term in radar images obtained with JPL airborne L-band SAR system," *IEEE Transactions on Geosci. and Remote Sensing*, Vol. 25, No. 1, 77–82, 1987.

3. Wang, J. R. and T. Mo, "The polarization phase difference of orchard trees," *International Journal of Remote Sensing*, Vol. 11, No. 7, 1255–1265, 1990.

4. Sarabandi, K., "Derivation of phase statistics of distributed targets from the Mueller matrix," *Radio Sci.,* Vol. 27, 553–560, Sep.–Oct. 1992.

5. Sarabandi K., Y. Oh, and F. T. Ulaby, "Measurement and calibration of differential Mueller matrix of distributed targets," *IEEE Trans. Antennas Propagation*, Vol. 40, 1524–1532, Dec. 1992.

6. Haldar, D., A. Das, S. Mohan, O. Pal, R. S. Hooda, and M. Chakraborty, "Assessment of L-band SAR data at different polarization combinations for crop and other landuse classification," *Progress In Electromagnetics Research B*, Vol. 36, 303–321, 2012.

7. Ulaby, F. T., K. Sarabandi, and A. Nashashibi, "Statistical properties of the Muller matrix of distributed targets," *IEE Proceedings F — Radar and Signal Processing*, Vol. 139, No. 2, 136–146, 1992.

8. Freeman, A. and S. L. Durden, "A three-component scattering model for polarimetric SAR data," *IEEE Transactions on Geosci. and Remote Sensing*, Vol. 36, No. 3, 963–973, 1998.

9. Freeman, A., "Fitting a two component scattering model to polarimetric SAR data from forests," *IEEE Transactions on Geosci. and Remote Sensing*, Vol. 45, No. 8, 2583–2592, 2007.

10. Toan, L. T., H. Laur, E. Mougin, and A. Lopes, "Multitemporal and dual-polarization observations of agricultural vegetation covers by X-band SAR images," *IEEE Transactions on Geosci. and Remote Sensing*, Vol. 27, No. 6, 709–717, Nov. 1989.

11. Kurosu, T., M. Fujita, and K. Chiba, "Monitoring of rice crop growth from space using the ERS-1 C-band SAR," *IEEE Transactions on Geosci. and Remote Sensing*, Vol. 33, No. 4, 1092–1096, Jul. 1995.

12. Toan, L. T., F. Ribbes, L. F. Wang, N. Floury, K. H. Ding, J. A. Kong, M. Fujita, and T. Kurosu, "Rice crop mapping and monitoring using ERS-1 data based on experiment and modeling results," *IEEE Transactions on Geosci. and Remote Sensing*, Vol. 35, No. 1, 41–56, Jan. 1997.

13. Hoekman, D. H. and B. A. M. Bouman, "Interpretation of C- and X-band radar images over an agricultural area, the Flevoland test site in the agriscatt-87 campaign," *International Journal of Remote Sensing*, Vol. 14, No. 8, 1577–1594, 1993.

14. Schotten, C. G. J., W. W. L. van Rooy, and L. L. F. Janssen, "Assessment of the capabilities of multi-temporal ERS-1 SAR data to discriminate between agricultural crops," *International Journal of Remote Sensing*, Vol. 16, No. 14, 2619–2637, 1995.

15. Freeman, J., J. D. Villasenor, H. P. Klein, and J. Groot, "On the use of multi-frequency and polarimetric radar backscatter features for classification of agricultural crops," *International Journal of Remote Sensing*, Vol. 15, No. 9, 1799–1812, 1994.

16. Ainsworth, T. L., J. P. Kelly, and J.-S. Lee, "Classification comparisons between dual-pol, compact polarimetric and quad-pol SAR imagery," *ISPRS Journal of Photogrammetry and Remote Sensing*, Vol. 64, 464–471, 2009.

17. Skriver, H., T. S. Morten, and A. G. Thomsen, "Multitemporal C- and L-band polarimetric signatures of crops," *IEEE Transactions on Geosci. and Remote Sensing*, Vol. 37, No. 5, 2413–2429, 1999.

18. Lee, J.-S., M. R. Grunes, and E. Pottier, "Quantitative comparison of classification capability: Fully polarimetric versus dual-and single-polarization SAR," *IEEE Transactions on Geosci. and Remote Sensing*, Vol. 39, No. 11, 2343–2351, 2001.

19. Turkar, V., R. Deo, Y. S. Rao, S. Mohan, and A. Das, "Classification accuracy of multi-frequency and multi-polarization SAR images for various land covers," *IEEE Journal of Selected Topics in Applied Earth Observations and Remote Sensing*, Vol. 5, No. 3, 936–941, Jun. 2012.

20. Panigrahy, R. K. and A. K. Mishra, "An unsupervised classification of scattering behaviour using hybrid polarimetry," *IET Radar, Sonar & Navigation*, Vol. 7, No. 3, 270–276, Mar. 2013.

21. Reigber, A. and O. Hellwich, "Radar tools homepage," http://adagio.bv.tu-berlin.de/rat; "IDL virtual machine," http://www.rsinc.com/vm, 2000.

22. Pottier, E. and C. Martines Lopez, http://earth.esa.int/PolSARpro, Version 4.2, 2011.